IRAQI JOURNAL OF APPLIED PHYSICS
Vol. 22, No. 1, January-March 2026, pp. 39-44

Suzan M. Shakouly [1]
GhazalaY. Hermiz [2]
Mahdi H. Suhail [2]

[1] Department of Physics, College of Education, AL-Mustansiriyah University, Baghdad, IRAQ
[2] Department of Physics, College of Science, University of Baghdad, Baghdad, IRAQ
* Corresponding author: suzanmalek2016@gmail.com

Calculation of Electric Field Generated by Mechanical Stress in $Bi_{1.8}Pb_{0.2}Sr_2Ca_2Cu_{3-x}Zn_xO$ Superconducting Thin Films

The mechanical properties of the $Bi_{1.8}Pb_{0.2}Sr_2Ca_2Cu_{3-x}Zn_xO$ superconducting films were prepared by pulsed-laser deposition (PLD) method. Shear force tests were performed on the prepared samples as a function of Zn concentration (x=0.2, 0.4, 0.6, 0.8, and 1). The characterization tests showed that the higher the Zn concentrations, the greater the strength of the sample to withstand the pressures, the break points of the sample were recorded at the maximum shear forces (2.5, 3, 5.7, 5.8, and 6.5 N) corresponding to Zn_x concentrations of (x=0.2, 0.4, 0.6, 0.8, and 1), respectively. The electrical properties of prepared $Bi_{1.8}Pb_{0.2}Sr_2Ca_2Cu_{3-x}Zn_xO$ thin film samples were measured by four probe technique to determine their critical temperatures for variable Zn concentrations and superconducting behavior, respectively. Some mechanical properties were theoretically and deeply studied based on the experimental results of shear force (0.5, 1, 1.5, 2, 2.5, 3, 3.5, 4, 5, 5.7, 5.8, 6, and 6.5N). Two values of stress were calculated; the first is the true stress, at which the sample fracture occurred, and the second is the geometric stress. Also, the work done to displace the perovskite lattice layers and the electric field generated by the effect of true stress between the layers were introduced. Finally, a model of the perovskite lattice $Bi_{1.8}Pb_{0.2}Sr_2Ca_2Cu_{3-x}ZnO$ was constructed to show the deformation caused by stress (piezoelectric deformation).

Keywords: Thin films; Shear force; Mechanical properties; Piezoelectric deformation model
Received: 26 April 2025; Revised: 10 July; Accepted: 17 July 2025; Published: 1 January 2026

1. Introduction

Superconductivity is the property of the certain materials to conduct DC electricity without energy loss when they are cooled below a critical temperature (T_C). These materials also expel magnetic fields as they transition to the superconducting state [1]. There are two types of superconductors. They are called Type I and type II. Type I superconductors transform abruptly from their normal state to superconducting state and vice versa at the transition temperature. These superconductors show complete Meissner effect below their transition temperature. Type II Superconductors which totally exclude low applied magnetic field, but only partially exclude high applied magnetic fields; their diamagnetism is not perfect but mixed in the presence of high fields [2].

The superconducting compounds exhibit very low flexibility and high brittleness. As a result, these materials have limited poor mechanical properties for practical applications. In industrial applications of high temperature superconductors, mechanical properties such as stiffness, fracture toughness, and hardness are as crucial as superconductivity properties such as critical temperature, critical current density, and critical magnetic field. Therefore, in studies on superconducting materials has become an important research area [3,4].

Hermize et al. [5] have studied mechanical properties (Vickers microhardness, Young modulus, Yield strength, fracture toughness and surface energy) for the superconducting system $Bi_{1.6}Pb_{0.4}Sr_{1.8}Ba_{0.2}Ca_2Cu_{3-x}Ni_xO_{10+\delta}$. The Vickers microhardness measurements have been carried out to examine the effects of Ni substitution at concentrations x (0, 0.8, 1, and 2). The results showed a deterioration of the mechanical properties with increasing concentration of Ni. Hermiz et al. [6] have studied the effects of pressure on the mechanical properties of $Bi_{1.6}Pb_{0.4}Sr_{1.8}Ba_{0.2}Ca_2Cu_{2.2}Ni_{0.8}O_{10+\delta}$ bulk samples. Mechanical measurements showed the variation of Vickers microhardness, Young modulus and Yield strength as a function of pressure for different loads. Increase in microhardness, Yong modulus and Yield strength was observed with increasing load from 0.3 to 0.9 GPa. Rahal et al. [7] have studied the mechanical properties of the bulk $(SnO_2)_x(Bi_{1.6}Pb_{0.4})Sr_2Ca_2Cu_3O_{10-\delta}$ samples prepared by the solid-state reaction method. Vickers microhardness measurements for these samples were carried out at room temperature as a function of the applied load, heating temperatures and dwell time. They demonstrated the behavior of the indentation size effect (ISE) of these composite materials and the estimation of real hardness values by applying Meyer's law, and the Hays and Kendell (energy dissipation) model and some mechanical parameters, such as Young's modulus, yield strength, fracture toughness, and brittleness index of fine hardness curves. They found that the combination of an appropriate concentration of $(SnO_2)_x$ nanoparticles proved effective in enhancing the mechanical

properties of superconductors. Safaran et al. [8] have prepared $Bi_{1.65}Pb_{0.35}Sr_2Ca_2Cu_3O_{10+y}$ by solid state reaction and ammonium nitrate precipitation methods. They focused on a microhardness measurements to calaculate and investigate the mechanical properties for all samples. Their results showed an increase in properties of prepared samples as the load is increased. Al-Jurani et al. [9] have studied the effect of adding SnO_2 nanoparticles (20-40nm) and microparticles (0.12-0.2μm) on the mechanical properties of superconducting $(SnO_2)_xBi_{1.7}Pb_{0.3}Sr_2Ca_2Cu_3O_{10+\delta}$ systems with different concentrations of SnO_2 (x=0, 0.1, 0.2, 0.4 and 0.6 wt.%). Their results showed that the microhardness decreases non-linearly with increasing applied load. Also, results of Young's modulus and Yield strength demonstrated a decrease with increasing applied load. Saritekin and Uzumcu [10] have studied the changes of microstructural, mechanical and superconducting features of bulk $Bi_{1.8}Pb_{0.2}Sr_2Ca_{1.8}Pb_{0.2}Cu_3O_y$ materials prepared at different milling time intervals (0.5h≤x≤ 8h). Vickers microhardness measurements showed that (Bi,Pb)-2223 bulk superconducting specimens exhibit typical ISE behavior depending on the presence of both elastic and plastic deformation in the system. The results obtained from the hardness measurements have been analyzed by using Meyer law, PRS model, MPRS model, elastic–plastic deformation model, and Hays-Kendall approach. The Hays-Kendall approach was identified as the most successful model in describing the mechanical properties of the samples. Khattar et al. [11] have investigated the impact of SmF_3 and LaF_3 on the mechanical properties of $Tl_{0.8}Hg_{0.2}Ba_2Ca_{2-x}R_xCu_3O_{9-\delta-y}F_y$ superconducting phases (especially the (Tl,Hg)-1223 phase) prepared by solid state reaction method, where R=Sm and La ,with $0<x<0.10$. Mechanical behavior was studied throughout Vickers microhardness measurements under varying loads ranging from 0.49 to 9.8N and time from 10 to 90s. The Vickers microhardness values of all superconducting samples vary unsystematically with La and Sm concentrations. However, for Sm and La at x=0.025, the highest values of microhardness were achieved and compared to the pure sample and all substituted samples. This indicated that LaF_3 and SmF_3 had a considerable impact on enhancing the micro hardness of the samples at low doping levels.

In 1880, Jacques and Pierre Curie discovered that pressure generates electrical charges in a number of crystals such as quartz and tourmaline. They called this phenomenon the piezoelectric effect. The industrial breakthrough came with piezoelectric ceramics, when scientists discovered that barium titanate adopts piezoelectric characteristics on a useful scale when an electric field is applied [12]. Piezoelectric ceramics have spontaneous polarization, the positive and negative charge concentration of the unit cells are separate from each other [13]. After polarization, most of the reorientations are preserved even without the application of an electric field. However, a small number of the domain walls are shifted back to their original position due to internal mechanical stresses. Polarons are quasiparticles that arise from the interaction between electrons or holes and the surrounding lattice of a material. When an electron moves through a crystal lattice, it can distort the surrounding atoms and creating a localized distortion that moves with electron [14].

Electromechanical coupling in superconducting systems refers to the interplay between electrical and mechanical phenomena, where changes in electrical properties influence mechanical behavior, and vice versa. This coupling is crucial in various applications, including superconducting magnetic bearing, high-speed transportation systems. He et al. [15] have proposed a physics-based trans-scale model of the superconducting transition of high pressure Nb_3Sn based on molecular dynamics (MD) simulations of Nb_3Sn crystals under high pressure. This model investigates the electromechanical coupling effect of Nb_3Sn and discussed the effect of grain boundary deformation on electromechanical coupling through simulations. Yu et al. [16] have analyzed the electromagnetic and mechanical behaviors of HTS racetrack coils, a 3D coupled electromagnetic–mechanical model is used to consider the effect of coil deformation and the strain dependence of critical current. The effectiveness of the coupling model is validated by comparing the numerical results with experimental data in the literature. A numerical simulation of a 3D HTS racetrack coil subjected to an external electromagnetic field is carried out using coupled and uncoupled models. These results indicate that the structure deformation can reduce the penetration depth of the screening current, and the hoop stress and strain are mainly concentrated on the circular part of the racetrack coil. Yong et al. [17] have proposed a numerical model of electromechanical coupling behaviors in HTS $(Re)Ba_2Cu_3O_{7-X}$ (REBCO) coil. This model has been verified and the simulation outcomes of the coil during magnetization were compared with the experimental outcomes.

Some Bi-containing materials, like certain perovskites and bismuth layered structure materials, exhibit both piezoelectric properties due to the presence of Bi^{3+} ions and their ion -pair electron. These materials are gaining for piezoelectric properties, which can lead to large polarization and high piezoelectric coefficient, adding Bi as a dopant in materials like PZT ceramics can optimize piezoelectric properties.

In this research, the mechanical properties of superconducting $Bi_{1.8}Pb_{0.2}Sr_2Ca_2Cu_{3-x}Zn_xO$ films have been studied from measurement of Shear force as a function of Zn_x concentration (x=0.2, 0.4, 0.6, 0.8 and 1). Also, the amount of shear force needed to break the sample and its relationship to the concentration of Zn

was shown where the fraction was made at maximum forces (2.5, 3, 5.7, 5.8, and 6.5N).

2. Experimental Work

A $Bi_{1.8}Pb_{0.2}Sr_2Ca_2Cu_{3-x}Zn_xO$ target was mounted inside vacuum chamber with 10^{-4} mbar and ablated by a 532nm Q-switched Nd:YAG pulsed laser at pulse duration of about 7 ns and energy density of 0.4-8 J/cm^2 focused on the target to generate plasma plume. All samples were grown on (111) Si substrates. Oxygen background pressure of 0.002 mbar was used. The $Bi_{1.8}Pb_{0.2}Sr_2Ca_2Cu_{3-x}Zn_xO$ samples were deposited at substrate's temperature (T_S) of 300 °C, annealing temperature (T_a) of 880 °C undergone for heat treatment in oxygen flow of 2 liter/min for 2 hours with heating rate of 15 °C/min.

Four probe dc method at low temperature was used to determine the critical temperature (T_C). The probe was connected to the surface of the film using conductive silver paste. The thickness (d) of the superconducting $Bi_{1.8}Pb_{0.2}Sr_2Ca_2Cu_{3-x}Zn_xO$ film was measured by optical interferometric method [18], to be equal to 184.2 nm for film length (L) of 1 cm.

3. Results and Discussion

When the sample is exposed to a shear force parallel to the surface, its length is deformed, without a change in the film thickness, so the true stress (σ_{tru}) can be calculated from the ratio of shear force to the instantaneous section area (A_i) of contact with the force.

In order to calculate the amount of deformation in length, from Fig. (1), the displacement of the sample is 1.2 mm, since the deformation causes an increase in the length of the film to 0.0112 m. So the instantaneous cross-sectional area (A_i) of the sample = dx1.2x10^{-3} m =0.221x10^{-9} m^2. The original area of the sample (A_0) equals to Lxd, So the value of A_0 is 1.842x10^{-9} m^2. Consequently, the geometrical stress (σ_{gE}) can be defined by the ratio of the shear force applied to the original unit area of the sample. Table (1) shows the values of shear force, true stress σ_{tru}, and geometrical stress σ_{gE}, for the prepared samples as functions of Zn_x concentration (x=0.2, 0.4, 0.6, 0.8, and 1)

Table (1) Values of geometrical stress σ_{gE} and true stress σ_{tru} of $Bi_{1.8}Pb_{0.2}Sr_2Ca_2Cu_{3-x}Zn_xO$ superconducting films at two different values of Zn concentration (x=0.2 and 0.4) and the amount of applied shear force (0.5, 1, 1.5, 2, 2.5, 3, and 3.5N)

x=0.2 T_C=93K F_{max}=2.5N	$\sigma_{gE} \times 10^8$ (Pa)	σ_{tru} 10^8 (Pa)	x=0.4 T_c=97k F_{max}=3N	$\sigma_{gE} \times 10^8$ (Pa)	$\sigma_{tru} \times 10^8$ (Pa)
0.5	2.26	2.46	0.5	2.26	2.46
1	4.52	4.93	1	4.52	4.93
1.5	6.78	7.40	1.5	6.78	7.40
2	9.04	9.87	2	9.04	9.87
2.5	11.31	12.33	2.5	11.31	12.33
3	13.57	14.80	3	13.57	14.80
3.5	15.83	17.27	3.5	15.83	17.27

The behavior of curves in Fig. (1) shows that the increase in applied shear force causes an increase in deformation and thus shear strain. We note that the parallel shear strength increases with increasing Zn concentration from 0.2 to 0.4. The initial shear force applied to the sample surface is 0.5 N and gradually increases by half until the maximum force at 3.5 N that the sample can withstand is reached.

For the concentrations of 0.6, 0.8, and 1 wt.%, the resistance of the sample to withstand the force increased. The first shear force is 4 N and gradually increases by 1 until we reach the highest shear value that the sample can withstand (6 N).

The work accomplished by the shear force for the displacement of the layers is equal to (shear force by displacement) increases with the increase in Zn concentration and the highest work accomplished by the force at displacement between 0.9 and 0.95mm. The reason is thought to be the CuZnO layer, which has little tensile strength, brittle and has little rigidity.

Table (3) Values of performed work, highest shear forces F_{max}, and corresponding displacement of force and values of the electric field generated from the effect of true stress σ_{tru} for different Zn concentrations (x=0.2, 0.4, 0.6, 0.8, and 1)

x (wt.%)	Displacement (mm)	F_{max} (N)	W x10^{-3} (J)	E x10^4 (V/m)
0.2	0.90	2.5	2.25	2.254
0.4	0.93	3.0	2.79	2.510
0.6	0.94	5.7	5.35	3.477
0.8	0.91	5.8	5.27	3.451
1	0.95	6.8	6.46	3.820

Table (3) and figure (2) show the work done by the maximum shear force (F_{max}) to move the layers as a function of Zn_x (x=0.2, 0.4, 0.6, 0.8, and 1) for $Bi_{1.8}Pb_{0.2}Sr_2Ca_2Cu_{3-x}Zn_xO$ superconducting films using the relationship W=F_{max} x displacement (mm).

We can make a connection between the mechanical and electrical properties to imagine that the layer CuZnO in $Bi_{1.8}Pb_{0.2}Sr_2Ca_2Cu_{3-x}Zn_xO$ perovskite lattice is a capacitor, Cu and O chains represent positive and negative plates, respectively, so the insulating layer between them is Zn concentration. In this case, the electric field lines are generated by stress springs from Cu plates and vanish at O plates.

The values of the electric field (E) generated by the effect of the true stress (σ_{tru}) between the layers of the perovskite lattice are calculated using the relationship W=½ $\varepsilon_r \varepsilon_0 E^2$, where W is the work done at the highest shear force (F_{max}), ε_0 is the electrical permittivity of vacuum (8.85x10^{-12} F/m), ε_r=1 is the relative electrical permittivity of Zn [19], which means that Zn does not change the electric field between charges as much as a vacuum does.

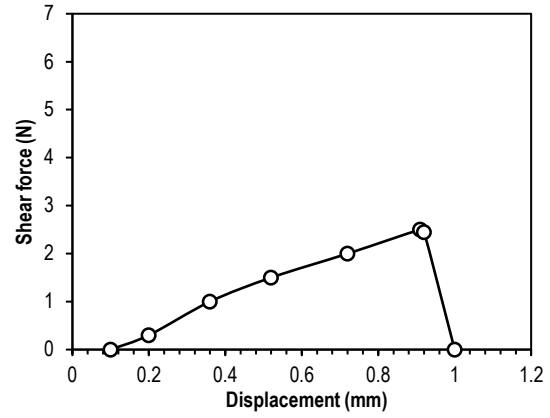

(a) x=0.2

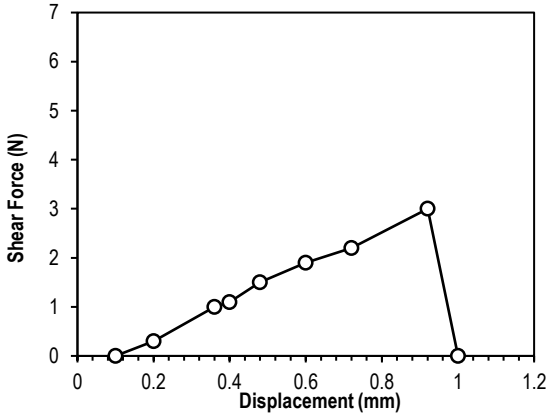

(b) x=0.4

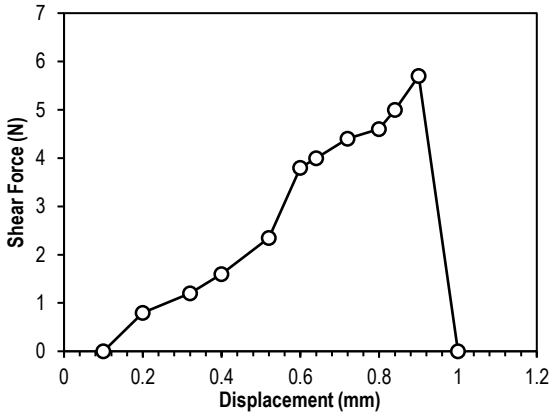

(c) x=0.6

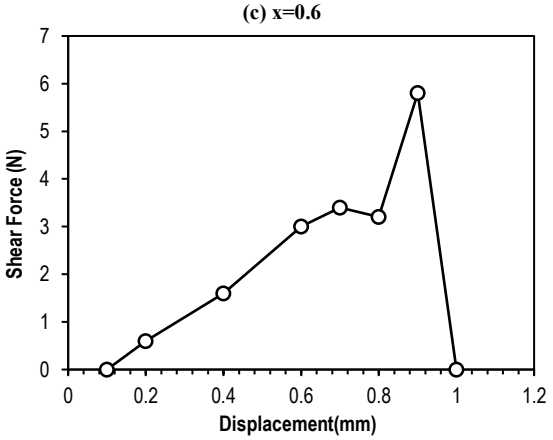

(d) x=0.8

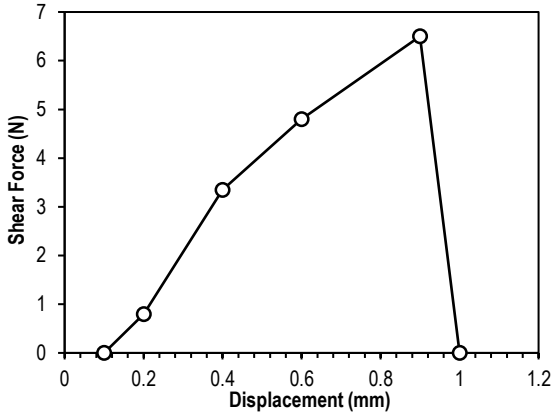

(e) x=1

Fig. (1) Shear force as a function of displacement of layers $Bi_{1.8}Pb_{0.2}Sr_2Ca_2Cu_{3-x}Zn_xO$ superconducting film for different Zn concentrations (x=0.2, 0.4, 0.6, 0.8, and 1)

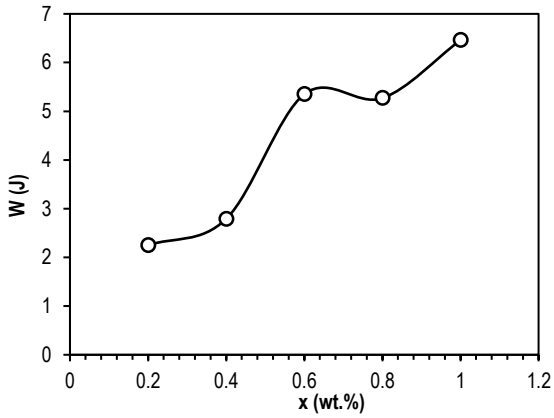

Fig. (2) Work performed to move perovskite lattice layers as a function of Zn concentration (x=0.2, 0.4, 0.6, 0.8, 1)

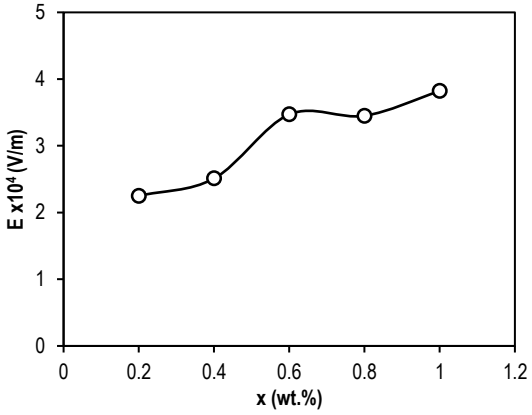

Fig. (3) Electric field generated by mechanical stress as a function of Zn_x at (x=0.2, 0.4, 0.6, 0.8, and1) for $Bi_{1.8}Pb_{0.2}Sr_2Ca_2Cu_{3-x}Zn_xO$ perovskite lattice

4. Conclusion

It can be concluded that the shear force acts in two opposite directions on the layers of the perovskite lattice, so there is a disturbance in the movement of the copper pairs and is accompanied by a piezopolaron particle resulting from the electron-phonon interaction and their association with each other when the

movement of electrons. When the electron moves through the atoms that make up the lattice, it causes the displacement of neighboring charges, moving away from it if the charges are negative and approaching it if they are positive, which causes a distortion in the distribution of charges as well as the emergence of a polarization zone that travels with the moving electron and returns to the normal state after crossing it. There is a polaron similar companion to the movement of the hole, which is the absence of an electron from the valence band, so the hole is treated as a moving particle, but it has a positive charge, so a double dipole occurs between the copper pairs and the polaron pairs, and as a result an electric field is generated. Figure (4) shows a schematic representation of a deformation model showing the displacement of perovskite lattice layers of a film by the action of a shear force parallel to the surface because of this, distortion occurs and thus the piezoelectric effect.

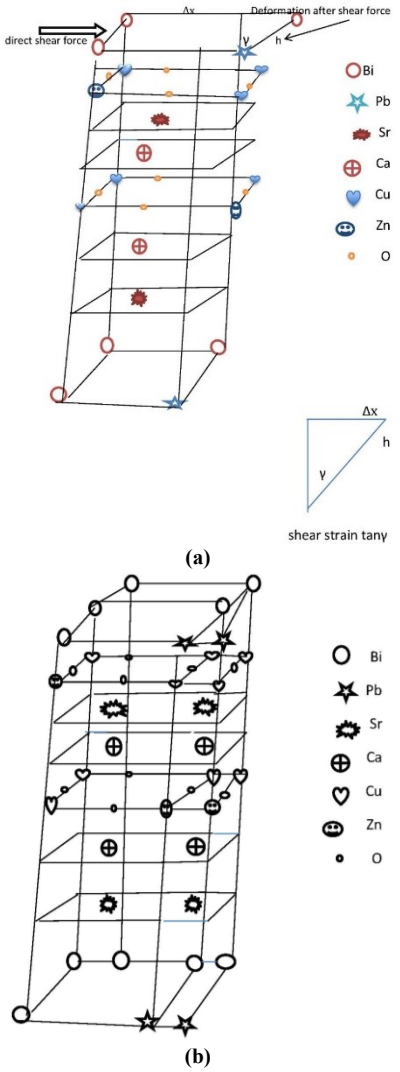

Fig. (4a,b) Schematic representation of the distortion model causing the piezoelectric effect in a $Bi_{1.8}Pb_{0.2}Sr_2Ca_2Cu_{3-x}Zn_xO$ perovskite lattice

References

[1] K. Fossheim and A. Sudbo, **"Superconductivity – Physics and Applications"**, John Wiley & Sons, Ltd. (2005).

[2] W. Meissner and R. Ochsenfeld, "Ein neuer Effekt bei Eintritt der Supraleitfähigkeit", *Naturwissenschaften*, 21 (1933) 787.

[3] N.K. Saritekin et al., "Mechanical and superconducting properties of Bi-based superconductors", *J. Mater. Sci.: Mater. Electron.*, 27 (2016) 956–959.

[4] R. Awad et al., "Influence of rare earth elements on the properties of Bi-based superconductors", *J. Supercond. Nov. Magn.*, 24 (2011) 1947–1956.

[5] G.Y. Hermiz, B.A. AL-Jurani and H.A. Thabit, "Mechanical properties of $Bi_{1\cdot6}Pb_{0\cdot4}Sr_{1\cdot8}Ba_{0\cdot2}Ca_2Cu_{2\cdot2}Ni_{0\cdot8}O_{10+\delta}$ superconducting system", *J. Supercond. Nov. Magn.* 25 (2012) 1629-1634.

[6] G.Y. Hermiz, B.A. AL-Jurani and H.A. Thabit, "Effect of pressure on the superconducting and mechanical properties of $Bi_{1\cdot6}Pb_{0\cdot4}Sr_{1\cdot8}Ba_{0\cdot2}Ca_2Cu_{2\cdot2}Ni_{0\cdot8}O_{10+}\delta$ system", *Adv. Mater. Phys. Chem.*, 3(1) (2013) 42–47.

[7] H.T. Rahal et al., "Structural and superconducting properties of Bi-based compounds", *J. Supercond. Nov. Magn.*, 30 (2017) 1971–1980.

[8] S. Safran et al., "Mechanical, microstructural and magnetic properties of the bulk BSCCO superconductor prepared by two different methods", *J. Mater. Sci.: Mater. Electron.* 26 (2015) 2622-2628.

[9] B.A. AL-Jurani, G.Y. Hermiz and M.N. AL-Dulaimi, "Study the effect of micro and nano particle size of SnO_2 on the mechanical properties of $(SnO_2)xBi_{1\cdot7}Pb_{0\cdot3}Sr_2Ca_2Cu_3O_{10+}\delta$ superconducting system", *Indian J. Nat. Sci.*, 7(42) (2017) 12348-12355.

[10] N.K. Saritekin and A.T. Uzumcu, "Investigations on the superconducting phases of Bi-based materials", *J. Supercond. Nov. Magn.*, 35 (2022) 2259–2273.

[11] R.F. Khattar et al., "Study of transport and structural properties in Bi-superconductors", *Cond. Matter*, 8(4) (2023) 87.

[12] D. Mihailovic, "Insights into the polaron physics of high temperature superconductors from optical and time-domain spectroscopy", *Physica C: Superconduct. Appl.*, 615 (2023) 1354385.

[13] S. Bhalla et al., **"Piezoelectric Materials"**, First Wiley (2016), ISBN: 9781119265139, DOI: 10.1002/9781119265139.

[14] R.A. Johnson, "Introduction to Electromechanical Filters", in **CRC Handbook of Electrical Filters**,

J.T. Taylor and Q. Huang (eds.), CRC Press (2020).

[15] Y. He et al., "Electromechanical coupling in high-pressured superconducting Nb_3Sn: analytical and simulation models", *Int. J. Mech. Sci.*, 230 (2022) 107541.

[16] L. Yu et al., "Electromagnetic-mechanical coupling analysis of high superconducting racetrack", *Supercond. Sci. Technol.*, 36(11) (2023) 115008.

[17] H. Yong et al., "Numerical modelling of electromechanical coupling behavior in HTS coil with implementation of H formulation in FE software", *Superconduct.*, 10 (2024) 100097.

[18] E. Hecht, **"Optics"**, Wiley (NY, 1998) p. 132.

[19] A.A. Mawla and S. Kim, "Experimental evaluation of bearing capacity using superconducting sensors", *Proc. 11th Int. Conf. on the Bearing Capacity of Roads, Railways and Airfields*, Taylor & Francis (2022).

Table (2) Values of geometrical stress (σ_{gE}) and true stress (σ_{tru}) of $Bi_{1.8}Pb_{0.2}Sr_2Ca_2Cu_{3-x}Zn_xO$ superconducting films at Zn_x x=0.6, 0.8, and 1, and the amount of shear force applied to the samples (4, 5, 5.8, 6, and 6.5N)

x=0.6,T_c=95K $F_{max=5.7\ N}$ F(N)	$\sigma_{gE} \times 10^8$ (pa)	$\sigma_{tru} \times 10^8$ (pa)	x=0.8,T_c=102K $F_{max=5.8\ N}$ F(N)	$\sigma_{gE} \times 10^8$ (pa)	$\sigma_{tru} \times 10^8$ (pa)	x=1 T_c=super behavior $F_{max=6.5}$ F(N)	$\sigma_{gE} \times 10^8$ (pa)	$\sigma_{trux} 10^8$ (pa)
4	18.090	19.74	4	18.090	19.740	4	18.090	19.740
5	22.620	24.67	5	22.620	24.670	5	22.620	24.670
5.8	25.790	30.94	5.8	26.244	31.487	5.8	26.244	31.487
6	27.149	32.50	6	27.149	32.500	6	27.149	32.500
6.5	29.411	35.28	6.5	29.411	35.280	6.5	29.411	35.280

